Sakarya Üniversitesi Fen Bilimleri Dergisi
Sakarya University Journal of Science

e-ISSN : 2147-835X
Publisher : Sakarya University

Vol. 29, No. 6, 735-759, 2025
DOI: https://doi.org/10.16984/saufenbilder.1733478

Research Article

The Assessment of Corrosion-Damaged Reinforced Concrete Structures: A Case Study from Erzincan, Türkiye

Ahmet İhsan Turan

Erzincan Binali Yıldırım University, Engineering and Architecture Faculty, Department of Civil Engineering, Erzincan, Türkiye, ahmet.turan@erzincan.edu.tr, ror.org/02h1e8605

ARTICLE INFO

Keywords:
Natural corrosion
Mechanical properties
Reinforced concrete structures
Reinforcing steel
Enviromentel effects

Article History:
Received: 03.07.2025
Revised: 06.11.2025
Accepted: 18.11.2025
Online Available: 14.12.2025

ABSTRACT

Reinforced concrete (RC) structures constructed in accordance with earthquake regulations and design principles are subjected to numerous effects, including wind, dead, live, snow, rain, seismic loads, and environmental effects on their service life. One of the most common problems caused by environmental effects is corrosion that occurs in the reinforced concrete reinforcement bar. Concrete can protect the reinforcement bar with sufficient strength and durability properties and undamaged cross-section integrity from corrosion under normal conditions. However, poor concrete quality, high permeability, insufficient concrete cover thickness, and workmanship defects can lead to corrosion of the reinforcement bars. Corrosion in the reinforcement bars can weaken the mechanical properties of the material and shorten the service life of the structure. In this study, the deterioration of concrete and reinforcement in a reinforced concrete structure built in 1982 in Erzincan was investigated using both destructive and non-destructive methods. The aim of examining these materials together was to evaluate the parameters affecting corrosion mechanisms at the material level as well. The results were interpreted by evaluating the climatic data (precipitation, humidity, wind, and temperature) and air quality at the structure's location. Qualitative and quantitative analyses revealed that the increasing corrosion rate causes deterioration in the mechanical properties of the reinforcement bars and that this deterioration is closely related to the type of corrosion. Additionally, it was concluded that the temperature differences and air pollution in Erzincan caused structural deterioration in reinforced concrete elements and accelerated corrosion of the reinforcement bars.

1. Introduction

Throughout their long service lives, RC structures may be exposed to various types of damage due to environmental factors such as high temperatures, acid attacks, carbonation, and corrosion, as well as mechanical stresses caused by earthquakes. It has been noted in several studies that one of the most common structural failures in reinforced concrete structures with service lives is the corrosion of the reinforcement bars [1-3].

Corrosion mechanisms are influenced not only by the material's microstructure but also by the chemical composition of the environment and by physical and mechanical actions [4]. Because these parameters directly control corrosion resistance and kinetics, different forms of corrosion develop under different exposure conditions [5]. Fontana (2005) [6] classifies eight forms: uniform corrosion, crevice corrosion, erosion-corrosion, galvanic corrosion, intergranular corrosion, selective leaching (dealloying), pitting corrosion, and stress-corrosion cracking (SCC).

Galvanic corrosion occurs when dissimilar metals are electrically connected in an electrolyte; the metal with the lower (more active) potential becomes the anode and corrodes, while the more noble metal acts as the

Cite as: A. İ. Turhan, "The assessment of corrosion-damaged reinforced concrete structures: A case study from Erzincan, Türkiye," Sakarya University Journal of Science, vol. 29, no. 6, pp. 735-759. https://doi.org/10.16984/saufenbilder.1733478

cathode [7, 8]. SCC develops under sustained tensile stress in a specific corrosive environment [9] and is relevant in sectors such as nuclear power generation [10]. Intergranular corrosion involves preferential attack at grain boundaries (e.g., after sensitization or precipitate formation), where boundary regions behave anodically relative to grain interiors [11]. Selective leaching (dealloying) is the preferential dissolution of the more active constituent from an alloy, leaving a porous, mechanically weakened residue [12]. Erosion corrosion is the synergistic material loss caused by combined electrochemical corrosion and mechanical wear due to flowing fluids and entrained particles [13]. In RC, corrosion of steel typically manifests as uniform corrosion following carbonation-induced depassivation or as pitting corrosion driven by chloride ingress through the cover or cracks.

The physical and chemical properties of concrete, its alkaline structure ($pH \geq 9$), and the adequate concrete cover, and low-porosity/low-permeability prevent corrosion from forming steel reinforcement in reinforced concrete (RC) structures under normal conditions. However, physical deterioration mechanisms such as wind-borne salts, acidic environments, and harmful components such as sulfate and chloride ions used in concrete production, carbonation seen in structures near coastal areas, and freeze-thaw cycles of concrete can weaken the material properties of concrete (e.g., yield stress, ultimate stress), eliminating the protective effect of the passive layer on the surface of the reinforcement, thus paving the way for the corrosion of the reinforcement bars [14, 15]. In RC structures exposed to these conditions, atmospheric corrosion is the most common form [16]. Atmospheric corrosion causes significant economic losses worldwide each year [17]. According to the World Corrosion Organization (WCO), it accounts for more than half of total corrosion-related damage [18].

The primary environmental parameters governing atmospheric corrosion rates include wind, temperature [19], humidity [20], and precipitation [21, 22]. Beyond these external effects, material-level factors in RC such as lower concrete pH (e.g. because of carbonation), higher permeability, and greater moisture availability also play a key role in the initiation and propagation of reinforcement corrosion [23].

Table 1 shows the relationship between pH level and the corrosion mechanism [23]. Some researchers have noted that temperature is not a directly dominant factor but plays an accelerating role in the corrosion process in the presence of prolonged humidity [24, 25].

Table 1. Corrosion and pH relationship [23]

pH value	State of reinforcement corrosion
Below 9.5	Commencement of steel corrosion
At 8.0	Passive film on the steel surface disappears
Below 7	Catastrophic corrosion occurs

In addition to these parameters, the carbon dioxide (CO_2) emitted by vehicles in densely urbanized areas, along with industrial emissions and harmful gases from highly industrialized regions such as carbon monoxide (CO), ammonia (NH_3), and hydrogen sulfide (H_2S), are among the principal factors that accelerate the corrosion mechanism [26]. Numerous studies have investigated the effects of environmental factors on atmospheric corrosion. Water, one of the main constituents of the atmosphere, functions as the electrolyte in corrosion reactions. Water in the environment accumulates on the surface of reinforcing steel through condensation and adsorption. The amount of moisture adsorbed varies with relative humidity and temperature [27]. Reinforcement bars corrode, especially in buildings exposed to humid environments over time [28].

Li et al. (2022) [29] emphasized that wind speed, precipitation, and relative humidity have a large effect on the corrosion rate, while air temperature and chloride deposition are less effective. Pei et al. (2021) [30] stated that precipitation is the most significant environmental factor affecting the atmospheric corrosion ratio, according to the data obtained from field studies. It was also found that relative humidity significantly increases the corrosion of reinforcement bars even under low or no precipitation conditions.

Determining the corrosion of reinforcement bars in RC structures and evaluating its effects on the bars' mechanical properties are critical for a reliable assessment of RC structural performance [31]. Corrosion reduces the cross-sectional area

of the bars and decreases their mechanical properties (e.g., yield strength, ultimate strength, ductility) as well as bond strength. At advanced stages, the volumetric expansion of corrosion products generates radial pressure at the steel–concrete interface, inducing tensile stresses in the cover; once these exceed the tensile capacity of concrete, longitudinal splitting cracks and cover spalling occur (Fig. 1), compromising the integrity of the RC member [32, 33]. Fig. 1 schematically illustrates the progression of corrosion, adapted from Beaujean et al. (2024) [34].

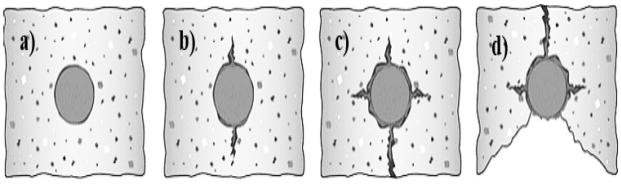

Figure 1. Progression of the corrosion process of the reinforcement bars in reinforced concrete: a) pre-corrosion, b) formation of corrosion products, c) occurrence of cracks, and d) spalling of the cover concrete [34]

In this context, these damage mechanisms significantly reduce the bond strength one of the main parameters determining the performance of reinforced concrete elements [35–37]. However, it has been reported that at very low corrosion levels, the bond strength can increase slightly: Tondolo (2015) observed increases of up to approximately 5% in the corrosion ratio, and Almusallam et al. (1996) observed increases of up to approximately 4%; above these thresholds, the bond decreases due to the volumetric expansion of rust products, cracking/splitting in the cover concrete, and weakening of the tightness of the bond [38, 39]. The literature (Esfahani & Rangan, 2018; Harajli, 2004) consistently demonstrates the positive effect of concrete compressive strength on the bond [40, 41].

Additionally, various experimental models predicting the effect of corrosion on bonding take into account major variables such as corrosion level, bar diameter, cover/diameter ratio (c/d_b), diameter/anchor length ratio, reinforcement yield strength, concrete compressive strength, and confinement provided by transverse reinforcement [42–44]. The types of damage described above can negatively impact the plastic hinge mechanism of reinforced concrete structures under potential seismic loads [45]. Consequently, reinforcement corrosion can shorten the service life of reinforced concrete structures and negatively impact both their structural integrity and functionality [46].

A review of the existing literature revealed that many studies have been conducted to predict the reduction in mechanical properties of both bare and concrete-embedded reinforcement bars after corrosion exposition. In a study conducted by Srivaranun et al. (2021) [47], reinforcement bars were exposed to either natural corrosion processes or accelerated corrosion techniques. Srivaranun et al. (2021) [47] have reported that natural corrosion processes and accelerated corrosion processes have both advantages and disadvantages over each other. Fernandez and Berrocal (2019) [48] have examined reinforcement bars exposed to natural corrosion in existing structures. In addition, previous experimental studies [49, 50] have proposed empirical models based on the corrosion ratio.

Field-based experimental studies on naturally corroded reinforcement bars allow a direct assessment of the environmental effects of concrete structures under actual service life conditions. However, there are limited data in the literature for such studies due to limitations such as the inaccessibility of the structures, the inability to take suitable samples, or the uncertainty of the corrosion level. Therefore, systematic field studies on reinforcement bars that have been exposed to corrosion in the natural environment for many years have the potential to make a significant scientific contribution to structural strength and material deterioration.

Yalciner et al. (2012) [51] investigated the corrosion mechanism in a 25-year-old school building. As a result of incremental pushover analyses performed by considering the deterioration in reinforcement and concrete, it was emphasized that corrosion negatively affects the service life and seismic performance of the structure. A 50-year-old high school building was analyzed by Yalciner et al. (2015) [52], considering its corrosion effects. In the relevant study, plastic hinges were modified as a result of corrosion effects and used in nonlinear pushover analyses. In light of the findings, a simple and

practical method for nonlinear seismic analyses to estimate the time-dependent performance levels of a 50-year-old corroded reinforced concrete building as a function of the corrosion rate was presented. Dasar et al. (2022) [53] investigated the corrosion rates in 40-year-old reinforced concrete beams that were exposed to tidal effects for 20 years and stored in a closed laboratory environment for another 20 years, and the structural performance of these elements was demonstrated by four-point bending tests. The corrosion status in reinforced concrete columns of a 41-year-old steel factory was investigated by Yao et al. (2022) [54], taking into account the design properties of the concrete and environmental effects such as temperature, relative humidity, CO_2 and SO_2 concentration, and the neutralization life for the concrete was calculated.

In this study, the corrosion of reinforcement bars in a reinforced concrete structure, which has been in service for 43 years and occurred as a result of various environmental and structural effects, was investigated in detail. Prior to the demolition process, we conducted both destructive and non-destructive tests on the concrete and the reinforcement bars of the structure. These tests were carried out to examine the structural factors that may affect the corrosion mechanism and their consequences. Furthermore, considering the location of the structure, climate, and weather data that may have an accelerating effect on the corrosion mechanism were obtained from various institutions. After the demolition of the building, the actual corrosion ratios were determined using the corroded reinforcement bars that were collected from the site, and the mechanical properties of these reinforcement bars were tested in the laboratory. In this context, the study contributes to the literature by revealing the effect of environmental factors on corrosion in a reinforced concrete structure that has been exposed to natural corrosion over time.

2. Materials and methods

This study involved both a field and a laboratory study. A summary of the studies carried out within the scope of field and laboratory work was shown in Fig. 2. More detailed information about these tests and visual inspections is provided in Sections 4. The field study was conducted in the Erzincan province, located in the Eastern Anatolia Region of Türkiye, in the RC structure shown in Fig. 3, which was built in 1982 and was used for different functions (flour factory and grain storage facility) over time.

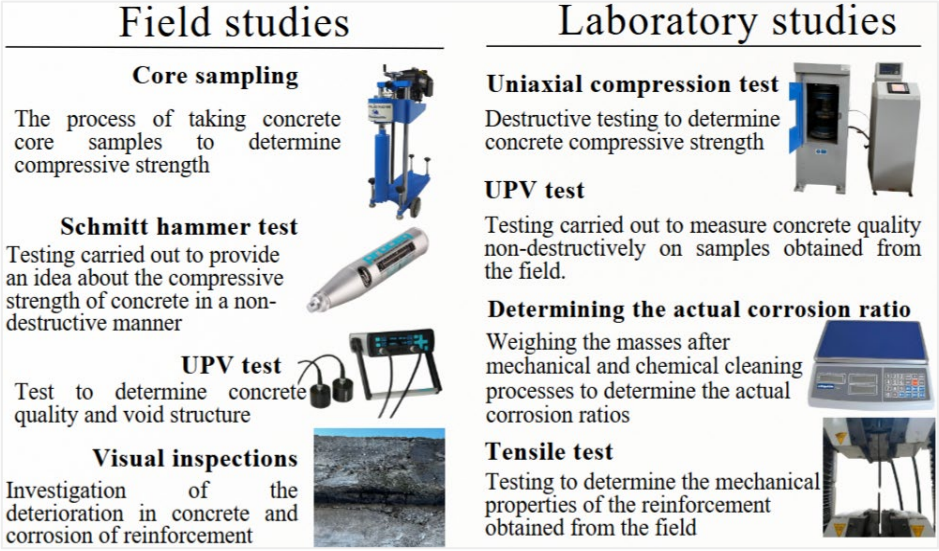

Figure 2. Conducted tests and visual inspections

Erzincan is located between 39º02″ and 40º05″ north latitudes and 38º16″ and 40º45″ east longitudes in an area that is characterized by a significant earthquake risk. The 1939 (Mw = 7.8) and 1992 (Mw = 6.8) earthquakes in Erzincan caused enormous loss of life and property [55, 56]. The earthquake in 1939 caused 32.968 deaths and 116.720 damaged buildings, while the earthquake in 1992 caused 653 deaths and 8.057 damaged buildings [57].

Figure 3. The section of the reinforced concrete structure that was examined during the field research and the demolition process

In this context, the environmental conditions, material properties, field observations, and laboratory tests were considered, and the parameters affecting the occurrence of the corrosion of reinforcement bars were investigated in a multifaceted manner.

3. Environmental Effects

RC structures may be subjected to structural deterioration over time due to hazardous environmental conditions (e.g., marine and acidic environments) and climatic effects (precipitation, humidity, and temperature changes) [58].

3.1. Environmental exposure conditions

In this study, meteorological data (annual precipitation amount, humidity percentage, and temperature changes) between 1982 and 2017 were obtained from the Erzincan Central Meteorological Station as detailed in Table 2.

The pollutant data that were used for the air quality assessment were obtained from the Air Quality Monitoring Stations operated by the Republic of Türkiye, Ministry of Environment, Urbanization, and Climate Change. These data can also be obtained from the National Air Quality Monitoring Network [59].

Table 2. Erzincan meteorological station

Station /Code	Erzincan/ 17094
District	City Center
ICAO	ERZC
OMGİ	151
Sensor	RSNY, TS, B
Observation Type	OMGI - Synoptic - Daily Air
Latitude	39°45'08.4"N
Longitude	39°29'12.6"E

OMGI: Automatic Meteorological Observation Station, RSNY: Wind, Temperature, Humidity, Precipitation, B: Pressure, Synoptic: A fundamental type of observation used for weather forecasting. All meteorological parameters are measured every three hours.

Temperature, relative humidity, precipitation, sulfur dioxide (SO_2), and particulate matter (PM10) levels were examined, and graphs showing monthly and annual changes in these parameters were analyzed to understand and evaluate the corrosion process. In this context, annual and seasonal effects of climatic variables such as temperature, humidity, precipitation, and air quality parameters were analyzed.

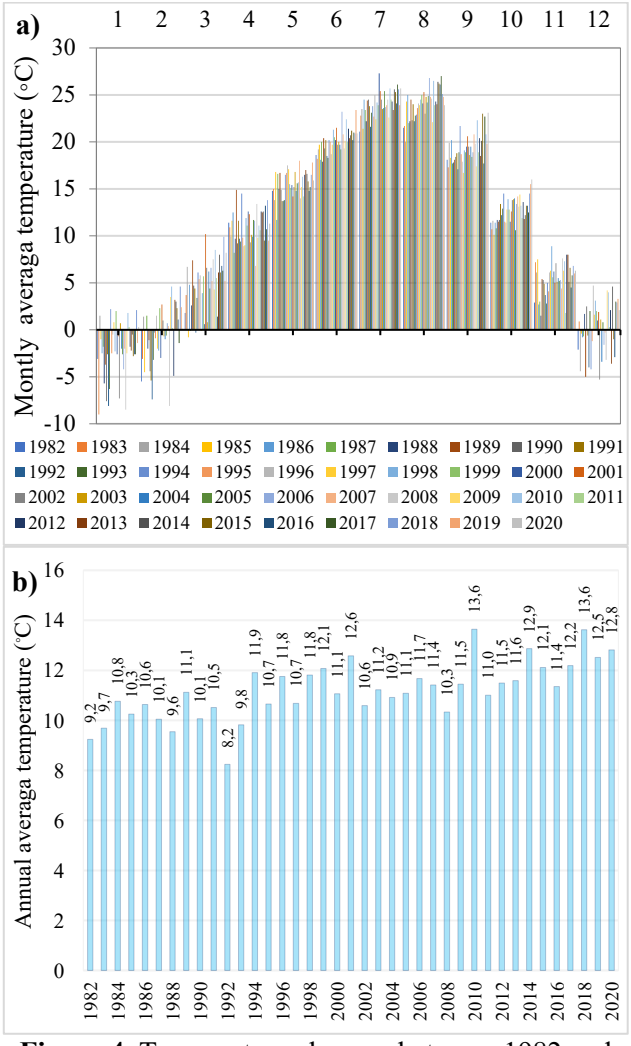

Figure 4. Temperature changes between 1982 and 2020: a) Monthly average temperature, and b) Annual average temperature

The two main time-dependent deformation components of concrete are shrinkage and creep [60]. Shrinkage behavior in concrete is an important parameter influencing its performance in climates with low humidity and large temperature variations. Moreover, temperature differences between seasons may adversely affect the durability of concrete structures and cause the formation of capillary cracks over time. Upon analyzing Figs. 4 and 5, it becomes evident that the summer months' low moisture content and high temperature changes exacerbate shrinkage deformations.

3.2. Effect of relative humidity and precipitation on corrosion

Many researchers have reported that the correlation between ambient humidity and corrosion ratio is non-linear [61-64]. Relative humidity (RH) is defined as the quantity of water vapor present in the air, expressed as a percentage of the amount that is necessary for saturation at the corresponding temperature [65]. RH is a significant environmental factor affecting the atmospheric corrosion process. Reviewing the existing literature, many studies have reported that an increase in RH increases the corrosion ratio [66-69]. It has also been noted that if the ambient relative humidity falls below the critical relative humidity (CRH) level, which varies depending on factors such as the type of material and the presence of salt ions in the environment, the corrosion mechanism becomes ineffective [70, 71].

Researchers have defined certain limit values for RH. Fig. 5 illustrates the changes in the monthly average RH between 1982 and 2017. It is seen that the RH values are high in the winter months and drop significantly in the summer months, leading to arid weather conditions. The increase in humidity in winter months, together with freeze-thaw events, can increase the permeability of concrete and pose a risk for the corrosion of reinforcement bars. The recurrent moisture cycles over many years are believed to induce deterioration in the mechanical properties of concrete.

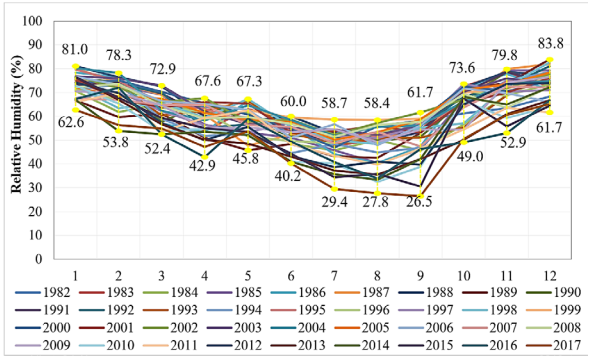

Figure 5. Monthly average relative humidity changes between 1982 and 2017

Precipitation may cause various harmful chemicals to leach into the reinforcement bars through the concrete cover, potentially deteriorating the mechanical properties of reinforced concrete elements. Besides the hazardous chemicals carried by precipitation, the duration and frequency of the precipitation are also important factors in this deterioration process [72].

An analysis of the monthly precipitation values revealed that they generally range between 20 and 60 mm, with high precipitation exceeding 100 mm in some years (Fig.6b.). Fluctuations in the precipitation regime can be decisive on the duration of exposure of concrete structures to environmental effects [58]. The highest annual average rainfall recorded was 52.2 mm in 1994, while the lowest annual average rainfall recorded was 20.7 mm in 1984 (Fig. 6b). The precipitation data shows that the annual average precipitation between 1982 and 2017 was 31.7 mm (Fig. 6b).

Besides the effect of precipitation during the winter months, freeze-thaw cycles may induce cracks to form on the concrete surface, rendering the reinforcement bars more vulnerable to the corrosion mechanism. During this process, water expands upon freezing, enlarging microcracks in the concrete and causing the loss of the protective layer around the reinforcement bars, which accelerates corrosion. In addition to climatic variables, air quality parameters were also analyzed. Air pollution caused by population density and industrial facilities has emerged as a serious environmental problem on a global scale.

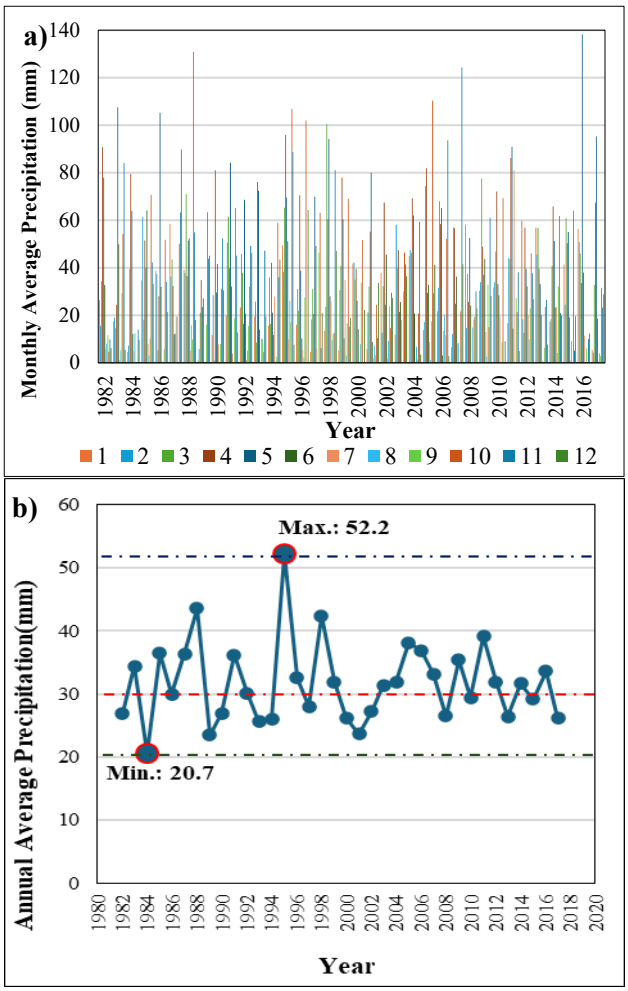

Figure 6. Changes in precipitation between 1982 and 2017: a) Monthly average precipitation, and b) Annual average precipitation

3.3. Air quality, atmospheric pollutant parameters and corrosion mechanisms

The Erzincan province, where the field study was conducted, is among the top 10 cities with the highest air pollution in Türkiye despite its low population density and lack of industrial facilities [73]. This adverse situation is reported to be primarily attributable to pollutant gases and the geographical characteristics of the province. The location of Erzincan in a plain surrounded by mountains, combined with the presence of a low inversion layer, increases the severity of air pollution caused by pollutant gases during the winter months (Erzincan Provincial Directorate of Environment and Urbanization, 2012) [74, 75]. In other words, the inversion layer leads to stagnant and windless weather conditions, preventing the upward dispersion of pollutant gases originating from the use of low-quality fuels for heating or from vehicle exhaust emissions, thereby causing polluted air to be trapped [76, 77].

The National Air Quality Index (AQI) is calculated based on five main air pollutant components. These pollutants are carbon monoxide (CO), particulate matter (PM10), nitrogen dioxide (NO_2), ozone (O_3), and sulfur dioxide (SO_2). The effect of atmospheric pollution on the corrosion process has already been emphasized. Sulfur dioxide (SO_2) reacts with water vapor (H_2O) in the atmosphere to form sulfurous acid (H_2SO_3) and then sulfuric acid (H_2SO_4) by oxidation. Furthermore, the damage intensity caused by sulfur dioxide has been found to be greater than that of other pollutants, with deterioration occurring in concrete, corrosion in reinforcement, and erosion effects [78].

These acids increase corrosion by accelerating chemical reactions on the reinforcement bars, which is the basic component of the reinforced concrete structure. Furthermore, sulfuric acid may decrease the pH level of concrete and disrupt the passive protective layer on the surface of the reinforcement bars, which poses a significant risk for corrosion. Therefore, determining the level of sulfur dioxide (SO_2) in the environment is crucial for understanding the corrosion of the reinforcement bars.

In certain standards (ISO 9224 [79]), the corrosion risks of materials exposed to air pollutants when metal surfaces are directly in contact with the atmosphere are presented along with the corresponding threshold values. In long-standing structures, especially when concrete undergoes time-dependent deterioration (e.g., spalling of the concrete cover, formation of cracks, etc.), reinforcement may also become directly exposed to the atmosphere. According to ISO 9224 (2012) [79], five different corrosion categories (C1–C5) are defined depending on atmospheric conditions. Additionally, the standard specifies an extra CX category corresponding to extreme corrosion associated with very high pollution or chloride content and prolonged humidity in tropical or subtropical regions (Table 3) Some researchers have also noted that the corrosion process is influenced by climatic factors such as humidity, temperature,

sulfur content, and salinity, as well as by pollutant gases [80, 81].

Tablo 3. Different corrosivity categories based on ISO9224 [79]

Categories	Corrosivity	Atmospheric Environments
C1	Very low	Dry or cold zone with very low pollution
C2	Low	$SO_2 < 5$
C3	Medium	$5 < SO_2$
C4	High	$30 < SO_2 < 90$
C5	Very high	$90 < SO_2 < 250$
CX	Extreme	$SO_2 > 250$

*Units in (g/m³)

An analysis of the monthly SO_2 concentrations for the Erzincan province based on the data between 2007 and 2024 revealed that the SO_2 concentration was high, especially in the winter season. This situation is attributed to emissions generated by the combustion of fossil fuels used for heating purposes [82]. As can be seen in Fig. 6a, it was determined that the average SO_2 concentration during the 17-year period was 10.11 µg/m³, while the minimum and maximum values varied between 0.92 µg/m³ and 43.71 µg/m³,respectively.

Particulate matter with diameters smaller than 10 µm is called PM10 [83]. Variations in PM10 concentrations are mostly due to anthropogenic emissions and meteorological factors [84]. The primary sources of PM10 include fuel consumption for transportation and heating, as well as waste from the construction and industrial sectors. PM10 can indirectly deteriorate concrete and reinforcement bars by transporting atmospheric contaminants, such as SO_2 and NO_2, to the concrete surface. As shown in Figure 7b, the annual changes in the PM10 levels were studied, showing an average of 63.38 µg/m³, with the lowest at 17.37 µg/m³ and the highest at 182.21 µg/m³.

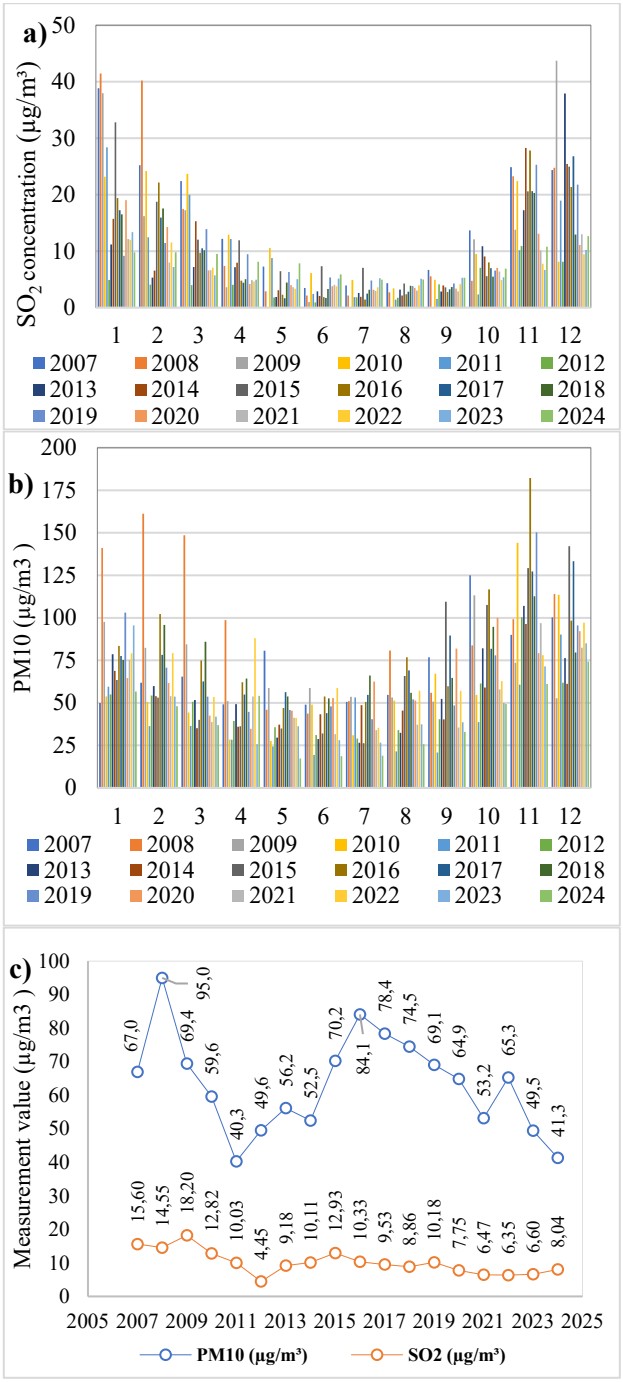

Figure 7. SO_2 and PM10 concentrations between 2007 and 2023: a) SO_2 concentration, b) PM10 concentration, and c) a comparison of SO_2 and PM10 values

Limits for these values are defined in various regulations. The World Health Organization (WHO) [85] has determined the annual average limit value for SO_2 as 20 µg/m³ and the annual average limit value for PM10 as 15 µg/m³. Considering these limit values, it is seen that the average SO_2 level obtained for the Erzincan province did not exceed the limits specified by WHO, but the PM10 level significantly exceeded the specified limit values. The limit values for air

pollutants in Türkiye are determined according to the provisions of the Air Quality Assessment and Management Regulation (AQAMR) (MoEU, 2008). Within the scope of efforts to improve air quality in Türkiye, the limit values defined for PM10 were revised from 300 µg/m^3 per day and 150 µg/m^3 per year in 2009 to 50 µg/m^3 per day and 40 µg/m3 per year in 2019 [86]. An analysis of Fig. 7b revealed that PM10 exceeded the limit values specified in the AQAMR. The efficacy of air pollution regulations in recent years is evident by the downward trend in the annual average values of PM10 shown in Fig. 7c.

4. Field and Laboratory Investigations

4.1. Field investigation

Field observations made on the reinforced concrete structure under investigation revealed various surface deteriorations over time. In RC structural elements, the depth of the concrete cover that surrounds the reinforcement and protects it from enviromental effects generally varies between 20 and 25 mm. As seen in Fig. 8, these deteriorations were manifested as biological formations, carbonation, and spalling of the concrete cover on the concrete surface.

It is observed that the coarse aggregates on the concrete surface have locally accumulated, leading to segregation. In the core samples, large rounded aggregates are evident (see Fig. 8e), which may cause bond problems at the mortar–aggregate interface. In addition, the segregation of fine particles is thought to caused honeycomb (see Fig. 8b), thereby increasing the permeability of the concrete.

The main causes of deterioration were inadequate material properties of the concrete, such as strength and permeability.

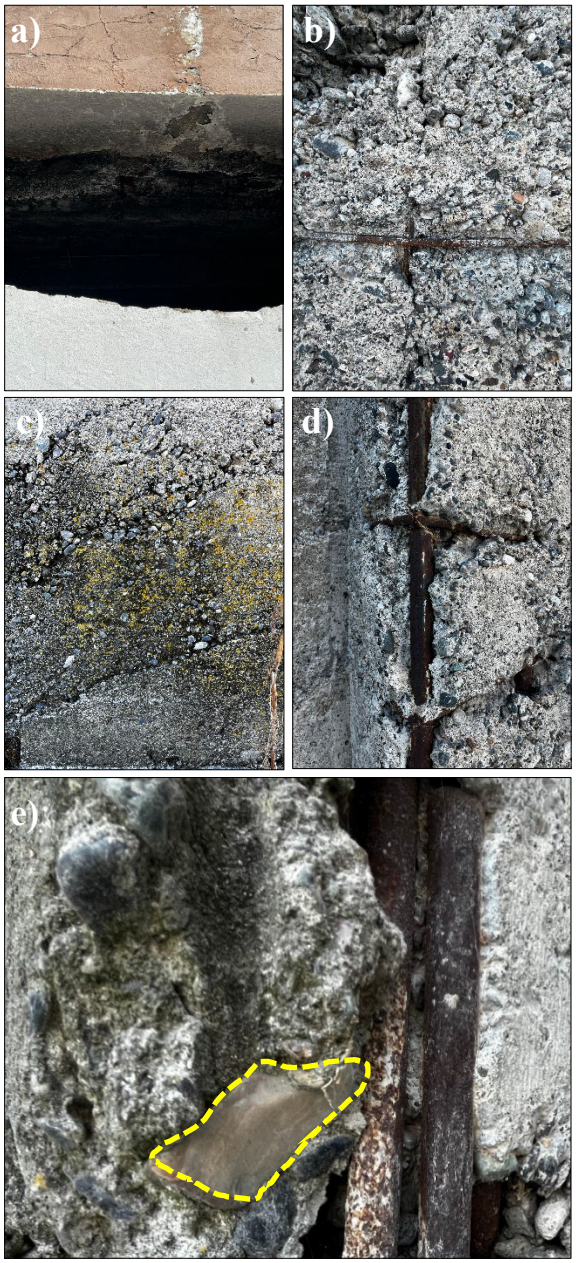

Figure 8. Observed deterioration types in the RC structure: a) carbonation, b) segregation, c) biological formations, d) corrosion, e) non granulometric aggregate distribution

Furthermore, the lack of widespread use of ready-mixed concrete during the building's construction period exacerbated the segregation problem. Elements without plaster or similar coating on the concrete surface left the structures unprotected against external environmental effects. The main parameters affecting the carbonation mechanism in concrete are water/cement (W/C) ratio, cement dosage, curing conditions, ambient humidity, temperature, and CO_2 concentration. These parameters also affect the strength of concrete after casting.

Both destructive (core sampling) and non-destructive tests (Ultrasonic Pulse Velocity [UPV] and Schmidt hammer) were carried out to determine the mechanical properties of the concrete.

Since RC columns are the most critical elements affected by curing conditions on construction sites, core samples were taken from these members. Before fixing the core drilling machine to the wall, the plaster layer was removed, and the core sampling area was identified using a rebar detection and localization device.

Non-destructive tests were performed on the RC columns from which core samples were taken. The destructive and non destructive tests performed on the samples taken from the structure are illustrated in Fig. 9.

Figure 9. Experiments performed on concrete samples obtained from the concrete structure: a) Core sampling, b) Schmitt hammer, c) UPV

The UPV method is used to determine the quality and homogeneity of concrete samples. The UPV values obtained depend on the pore structure, density, and mechanical properties of the concrete [87, 88]. The lengths of the core samples are divided by the measured transit times to calculate the ultrasonic transit velocities (Eq.1).

$$V = \frac{L}{T} \quad (1)$$

In Eq.1, V is the ultrasonic transmission velocity (m/sec or km/sec), L is the distance traveled by the waves (m or km), and T is the time duration (in seconds). In studies conducted by Whitehurst (1951) [89], limit values of ultrasonic transmission velocities were determined for concretes with a density of approximately 2400 kg/m³, and the concrete quality was classified using these values. Table 4 illustrates these limits.

Table 4. Concrete quality classification based on the UPV method [52]

Quality	Speed value
Very good	>4500 m/s
Good	3500-4500 m/s
Suspicious	3000-3500 m/s
Weak	2000-3000 m/s
Very weak	<2000 m/s

Post-field investigations on the reinforcement bars removed from the reinforced concrete structure revealed pitting and homogeneous corrosion types (Fig. 10). Fig. 10 illustrates the differences in the corrosion types identified in the field study. The volumetric expansion occurring in pitting corrosion is at a lower level compared to homogeneous corrosion. Therefore, the risk of the detachment of reinforced concrete from the concrete cover is higher in the case of homogeneous corrosion [89].

Figure 10. Corrosion types observed in the extracted reinforcement bars: (a) uniform corrosion and (b) pitting corrosion

Following the demolition of the reinforced concrete structure, a total of 50 reinforcement bar samples were obtained from the site. These samples consisted of 39 reinforcement bars with a diameter of 8 mm, 5 reinforcement bars with a diameter of 10 mm, and 6 reinforcement bars with a diameter of 12 mm. The reinforcement bar samples were prepared according to the appropriate tensile lengths specified in the TS EN ISO 15630-1 [90] standard. Considering the period when the structure was constructed, it was determined that the obtained reinforcement bars were smooth. Fig. 11 presents the reinforcement bars and the images after the cutting process.

Figure 11. Tensile test samples were taken from the reinforced concrete structure and prepared according to TS EN ISO 15630-1 [90]

4.2. Laboratory test methods

4.2.1. Material tests

To determine the compressive strength of the RC structure, 15 core samples taken from columns were cut to a length/diameter ratio of 2:1 using the core cutting machine shown in Fig. 12.

Figure 12. Concrete compressive strength testing: (a) core cutting, (b) testing machine, (c) compression test

The core samples, cut to appropriate dimensions, were allowed to dry in a laboratory environment. In the uniaxial compression tests, load transfer plates were used to ensure the smoothness of the sample head surfaces and to prevent negative effects on load transfer. Uniaxial compressive strength tests of the samples were conducted on a 2000 kN loading capacity machine, and a constant loading rate of 0.6 MPa/s was applied to the samples until the moment of failure in accordance with the EN 12390-3 [91] standard.

Following the compressive strength tests, we conducted UPV tests to assess the internal structural homogeneity of the structure. Considering the year in which the existing structure was built, it is understood that the concrete had a heterogeneous structure due to the concrete production and casting technologies used. This situation resulted in varying values in the UPV measurements conducted in the field experiment, contingent on the location of the measurements. The UPV tests shown in Fig. 13 were also performed on the core samples taken from the field experiment using the Pundit Lab device to minimize these differences.

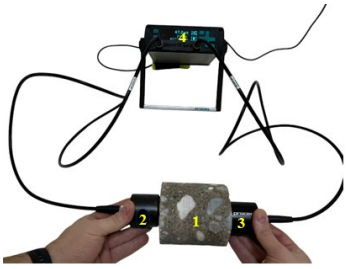

1: Concrete sample, 2: Receiver end, 3: Transmitter end, and 4: Measuring device

Figure 13. UPV test setup

Tensile testing was conducted alongside concrete tests to ascertain the mechanical behavior of the reinforcement bars. Tensile tests were performed in a laboratory setting to ascertain the mechanical properties of the reinforcement bars (Fig. 14). The tests were conducted in accordance with the TS EN ISO 15630-1 [90] standard, and the basic mechanical properties of the reinforcement bars, such as tensile strength, yield strength, and ultimate strain, were evaluated.

Figure 14. Tensile strength test

In structural engineering, reinforcement quality is generally examined in terms of mechanical properties such as yield strength, tensile strength and elongation [92].

4.2.2. Actual corrosion measurement method

The actual corrosion rates of the reinforcement bars were calculated using Eq.2, taking into account the initial (M_i) and final (M_f) mass values. To represent the initial mass, reinforcement bars that were not exposed to corrosion in the structure were used as a reference.

$$CL = \frac{M_{i-}M_f}{M_i} \times 100 \quad (2)$$

In the equation, M_i is the uncorroded mass of the reinforcement bars before corrosion (g) and M_f is the final mass of the reinforcement bars after cleaning the corrosion products (g). The corrosion rate is calculated using the section loss (ΔA_s) in the final reinforcement bars, as shown in Eq.3:

$$\Delta A_s = A_s \times \frac{\Delta m}{m} \quad (3)$$

In this calculation, A_s represents the nominal cross-sectional area of the reinforcement bars that non-corroded (mm^2).

Mass measurements were conducted by weighing the corrosion products on the reinforcement bars using a precision balance after mechanical cleaning. Uncorroded and homogeneous diameter reinforcement bar samples were used as a reference. This method aims to directly determine the numerical effect of corrosion in a laboratory environment.

5. Results and Discussion

This section offers a thorough examination of corrosion rates, the mechanical properties of the reinforcement bars, and concrete performance derived from the collected experimental data. The effect of corrosion on the cross-section and mechanical properties of the reinforcement bars, together with its consequences for the structural integrity of reinforced concrete structures, is examined. The results are based on direct measurements and compared assessments with existing literature.

5.1. The actual corrosion ratio

To identify the actual corrosion rates of the reinforcement bars obtained from the reinforced concrete structures, all the reinforcement bars were subjected to the physical and chemical cleaning processes shown in Fig. 15, in accordance with the methods specified in the ASTM G1-03 (2003) [93] standard. The primary purpose of these processes is to remove residues (e.g., concrete and rust) from the surface of reinforcement bars that could affect mass loss. In the first stage, mortar and rust residues on the reinforcement bars were cleaned using a wire brush. The reinforcement bars were then immersed in a Clark solution (approximately 50% HCl + 0.5% $SnCl_2$) for chemical cleaning.

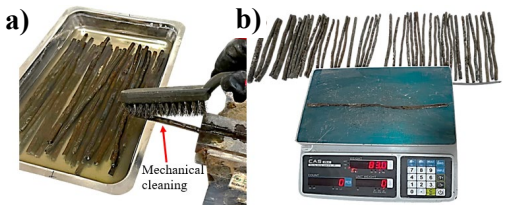

Figure 15. The process for obtaining actual corrosion rates includes: a) chemical and mechanical cleaning, and b) weighing the reinforcement bars

Table 5 presents the actual corrosion ratio obtained after the cleaning and weighing processes. According to the obtained results, the corrosion rates observed in the 8 mm diameter reinforcement bars exhibited a fairly wide distribution (6.33-29.87%). This result indicates that the insufficient thickness of the rust allowance exposes thin reinforcement bars to a higher rate of environmental factors. The 12 mm diameter reinforcement bars showed a lower minimum value (9.81%) with an upper limit of 25.57%, indicating that the passive layer was severely dissolved in some areas. These results suggest that reinforcement bars, especially those located in the external environment with insufficient passage allowance, may undergo rapid corrosion.

5.2. Mechanical properties of corroded smooth reinforcement bars

Tensile tests were performed in the laboratory in accordance with the ASTM A370-08 (2008) [94] standards to evaluate the mechanical properties of the reinforcement bars with the determined corrosion rates. Fig. 16 and Table 4 show the stress-strain data that were obtained from the tests. As seen in Fig. 16, the tensile strength and strain capacity of the reinforcement bars decreased significantly as the corrosion rate increased. Especially in the samples with pitting corrosion, significant decreases in yield and ultimate strain were recorded.

Table 5. Actual corrosion rates (C_L%) and cross-sectional area losses (ΔA_s) of the reinforcement bars with different diameters

No	D(mm)	W_i (gr)	W_f (gr)	C_L (%)	$\Delta As(mm^2)$
#1	8	118.5	92.3	22.11	14.27
#2	8	118.5	108.7	8.27	4.53
#3	8	118.5	92.5	21.94	14.13
#4	8	118.5	101.7	14.18	8.30
#5	8	118.5	98.1	17.22	10.45
#6	8	118.5	100.7	15.02	8.89
#7	8	118.5	83.1	29.87	21.41
#8	8	118.5	87.9	25.82	17.50
#9	8	118.5	111	6.33	3.40
#10	8	118.5	101.3	14.51	8.53
#11	8	118.5	106.2	10.38	5.82
#12	8	118.5	103.5	12.66	7.28
#13	8	118.5	108.5	8.44	4.63
#14	8	118.5	90.8	23.38	15.33
#15	8	118.5	100.6	15.11	8.94
#16	8	118.5	96.1	18.90	11.72
#17	8	118.5	87.7	25.99	17.65
#18	8	118.5	100.1	15.53	9.24
#19	8	118.5	87.7	25.99	17.65
#20	8	118.5	100.8	14.94	8.83
#21	8	118.5	90.3	23.80	15.70
#22	8	118.5	99.7	15.86	9.48
#23	8	118.5	92.4	22.03	14.20
#24	8	118.5	91.2	23.04	15.05
#25	8	118.5	109.2	7.85	4.28
#26	8	118.5	100.7	15.02	8.89
#27	8	118.5	89.9	24.14	15.99
#28	8	118.5	110.3	6.92	3.74
#29	8	118.5	104.2	12.07	6.90
#30	8	118.5	89.8	24.22	16.06
#31	8	118.5	98.8	16.62	10.02
#32	8	118.5	93.9	20.76	13.17
#33	8	118.5	108.5	8.44	4.63
#34	8	118.5	101.6	14.26	8.36
#35	8	118.5	100.8	14.94	8.83
#36	8	118.5	95.5	19.41	12.11
#37	8	118.5	96.9	18.23	11.20
#38	8	118.5	124.9	7.17	3.88
#39	8	118.5	144.5	15.19	9.00
#40	10	185.1	158.3	14.65	13.30
#41	10	185.1	168.8	8.81	7.58
#42	10	185.1	162.1	12.30	11.14
#43	10	185.1	240.2	15.72	14.65
#44	10	185.1	177.8	10.86	9.57
#45	12	264	220.2	16.59	22.50
#46	12	264	213.9	18.98	26.49
#47	12	264	238.1	9.81	12.30
#48	12	264	198.9	18.56	25.78
#49	12	264	100.7	25.57	38.85
#50	12	264	89.9	28.07	44.13

An analysis of the curves in Fig. 16 showed that the reference reinforcement bars with 0% corrosion reached the highest yield and ultimate strain values, while these values decreased significantly in the reinforcement bars with a 25.57% corrosion ratio.

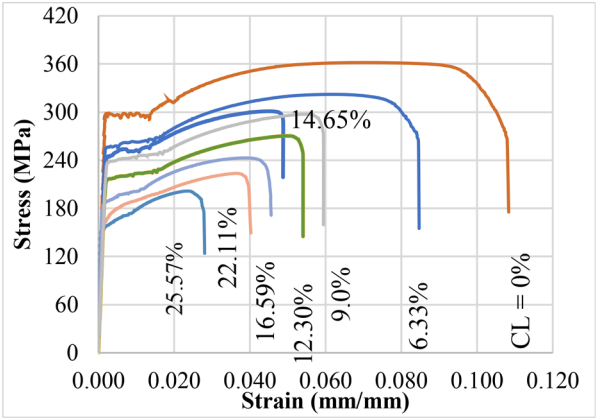

Figure 16. Stress-strain curves of the smooth steel reinforcement bars with different corrosion ratios

For example, as the corrosion ratio increased, the maximum stress level decreased from 370 MPa to approximately 190 MPa, while the ultimate strain dropped from 11% to less than 3%.

Table 4. Effect of corrosion level on mechanical properties of smooth reinforcement bars

#	Cl, (%)	Ø (mm)	*Fy*, (MPa)	*Fu*, (MPa)	ε_y (mm/mm)
Ref.	0	8	300	370	0.0015
1	6.33	8	280	335	0.0014
2	9.00	8	260	310	0.0013
3	12.30	10	240	285	0.0012
4	14.65	10	220	265	0.0011
5	16.59	12	200	245	0.0010
6	22.11	8	180	215	0.0009
7	25.57	12	160	190	0.0008

Figure 17 shows the corrosion-induced reductions in the cross-section of the 8 mm diameter reinforcements shown in Table 4. A notable observation is that, in specimens with low corrosion levels, the loss in cross-section is generally distributed homogeneously. As the corrosion level increases, localized constrictions in the specimen cross-sections become more pronounced.

After mechanical and chemical cleaning, the reinforcement bars were weighed to determine the mass loss. The results are presented in Tables 5.

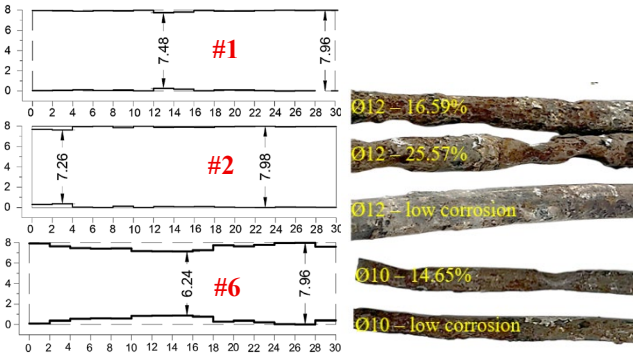

Figure 17. Cross-section reductions caused by corrosion

This result indicates a sudden weakening of the section of the reinforcement bar due to the effect of pitting corrosion and a reduction in ductility capacity. In the samples with homogeneous corrosion, these reductions were more stable. Similarly, Yalciner et al. (2020) [95] reported that increasing corrosion ratios directly affect the tensile capacity and strain behavior, and especially pitting corrosion causes stress concentrations. The data presented in Fig. 15 indicates that increasing corrosion levels have a direct effect on the strength and ductility of the reinforcement bars. Especially at corrosion ratios above 22%, the reinforcement bars started to display brittle fracture behavior, and the strain capacity decreased below 3%. This result indicates that the loss of ductility in corroded structural elements should be accounted for not only in terms of strength but also in terms of earthquake performance.

5.3. Concrete performance

To evaluate the current performance of the concrete, both destructive and non-destructive tests were performed, and the obtained results were compared with the requirements of the regulations.

In this context, UPV and Schmidt hammer tests were carried out in the field and in the laboratory. Table 6 presents the results of these tests and 8 core samples that were tested in the laboratory. According to the Regulation on Structures to be Built in Disaster Zones (RSBDS 1975), which was in force at the time that the building was constructed, for buildings with an importance factor >1, the minimum concrete strength requirement in 1st and 2nd degree zones was B225 (C18) [96].

Since the Erzincan province was a 1st degree earthquake zone at that time, concrete with a compressive strength of at least 20 MPa was required to be used in the structure. In the current Turkish Building Earthquake Code (TBEC 2018) [97], the use of at least C25 class concrete is mandatory for all reinforced concrete structures. Considering both the current earthquake code (TBEC 2018) and the code in force when the structure was built (RSBDS 1975), the concrete compressive strength of 7.16 MPa found in the structure was insufficient for the structural adequacy of the structure.

Fig. 18 illustrates the fracture types of different core samples after uniaxial compression tests. The conical, comminuted, and horizontal fracture types in the samples reflected the heterogeneous structure of the concrete and the differences in compressive strength.

Figure 18. Different types of crack and damage observed in core samples after uniaxial compressive testing

Table 6. UPV, Schmidt, and uniaxial compressive strength test results obtained in the field and laboratory environments

No	Ultrasonic Pulse Velocity (m/s) *	Ultrasonic Pulse Velocity (m/s)**	Schmidt Rebound Number	CS (MPa)
1	2610	2500	23	6.6
2	2786	2800	26	9.3
3	2803	2950	25	8.3
4	2752	2650	27	10.5
5	2466	2500	18	4.3
6	2540	2400	21	5.5
7	2600	2510	23	6.7
8	2440	2300	22	6.1

* Field measurement, **Lab. measurement (core sample), CS: Compressive strength

A analysis of Table 6 and Fig. 19 revealed that the UPV tests conducted in the field and the UPV measurements performed on the core samples in the laboratory generally yielded similar results. Differences in some measurement results are attributed to the age of the concrete, moisture content, and sample homogeneity.

In experimental studies aiming to determine the compressive strengths of concrete using non-destructive methods, a significant correlation was found between UPV measurements and concrete quality. Researchers have examined the correlation between the UPV data obtained from experimental studies and the compressive strengths of concrete and have developed various experimental models in line with this.

A strong correlation of $R^2 = 0.93$ was found between UPV field and laboratory measurements. This result supports the reliability of in-situ measurement techniques and demonstrates their usability in concrete performance assessments.

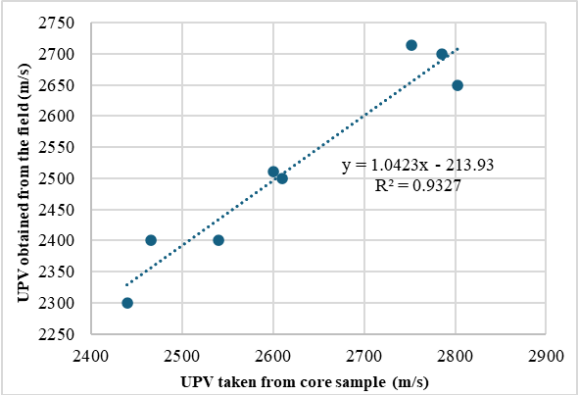

Figure 19. Classification of concrete quality according to the UPV values

An analysis of the correlation between concrete compressive strengths and the UPV results presented in Fig. 20 revealed a linear correlation between the two parameters. This result is consistent with many studies in the literature [98, 99].

Figure 20 shows a moderate correlation ($R^2 = 0.76$) between the concrete strength and UPV values. The fact that all the data correspond to "doubtful" or "medium" quality concrete ranges indicates that the structure was built with low-grade concrete. Non-destructive and destructive tests revealed that the concrete quality did not meet the requirements of the current regulations. UPV, Schmidt hammer, and compressive strength data were evaluated together and the performance level of the structure was supported by scientific and technical results.

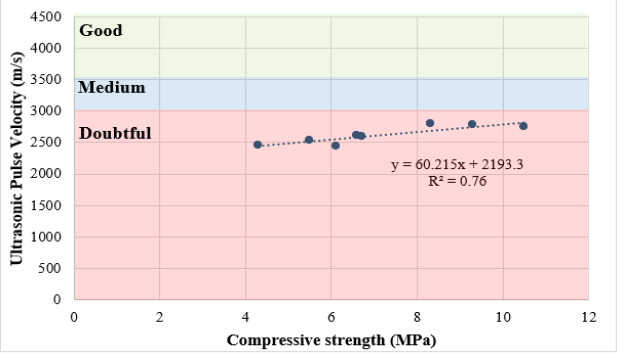

Figure 20. The correlation between UPV and concrete compressive strength values

6. Reinforcement corrosion and concrete quality in Erzincan RC structures

Corrosion in RC structures leads to a reduction in the target performance levels anticipated during the design stage due to the problems it causes.

6.1. Field investigations after the March 13, 1992 Erzincan earthquake

Although reinforced concrete structures are detailed in accordance with code requirements during the design stage, deficiencies and mistakes in on-site applications can lead to severe damage under possible seismic loads. One of the common on-site mistakes involves processes that directly affect concrete quality (such as insufficient compaction, rounded river aggregates) reinforcement bar corrosion or the use of hand-mixed concrete instead of ready-mixed concrete.

In this context, with Circular No. 248 issued by the Ministry of Public Works and Settlement in 2004, hand-mixed concrete casting was prohibited, and the use of ready-mixed concrete was made mandatory. However, prior to this regulation, hand-mixed concrete was widely preferred. The corrosion of poor quality concrete or reinforcement in buildings that were severely damaged or collapsed after the earthquake was demonstrated in many earthquakes, including the March 13, 1992 Erzincan earthquake.

Researchers conducted field investigations [100–105] following the M_w = 6.3 earthquake in Erzincan on March 13, 1992. In the field study carried out by Williams et al. (1992) [103], it was reported that corrosion was present in heavily damaged RC structures (see in Fig. 21).

In terms of concrete quality, researchers stated that low-quality concrete was used, honeycomb-like voids and segregated regions were observed in the concrete, and rounded aggregates were frequently identified [103, 104].

Furthermore, evaluations conducted on the damaged reinforced concrete structures emphasized that the concrete compressive strength was approximately 10 MPa [105, 106]. Ersoy (1992) [107] reported in his post-earthquake investigations that he observed poor concrete quality, inadequate concrete mixes, and segregation. Considering that the average concrete compressive strength of the reinforced concrete structure examined in this study was determined to be 7.16 MPa, it is evident that the concrete quality is even lower than that reported in post-earthquake field investigations.

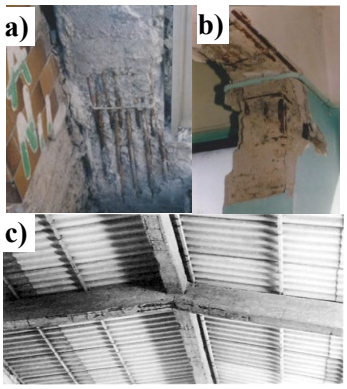

Figure 21. Corrosion damage in RC structures following the 1992 earthquake: (a) longitudinal bar corrosion in a column, (b) combined longitudinal and transverse bar corrosion in the beam–column joint, and (c) corrosion in a RC beam member [103]

Cengiz (1993) [108] reported the adverse effect on concrete quality when sand containing a high amount of silt, obtained from the Euphrates River, is used in concrete production. Uğurlu (2013) [109] emphasized that segregation caused by hand-mixing instead of ready-mixed concrete reduces the bond strength at the rebar–concrete interface. In the study conducted by Tekel (1996) [110] conducted a field study in 1996 stated that although approximately four years had passed since the earthquake and there were ready-mixed concrete production facilities in the city, concrete

production was still carried out, at least partially, by hand-mixed at construction sites.

Furthermore, it was reported that hand-mixed concrete produces structures with poor impermeability, allowing water penetration that promotes corrosion. In another study comparing hand-mixed and ready-mixed concretes, it was shown that compressive strengths obtained from hand-mixed concrete samples exhibited irregular distribution [111]. In the study conducted by Abosrra et al. (2011) [112], it was reported that as the concrete compressive strength increased from 20 to 46 MPa, the corrosion rate decreased. Field investigations have also shown that corrosion is frequently observed in structures with low concrete compressive strength [113–115].

As can be understood from the presented information, voids formed in the concrete structure due to hand-mixed concrete in long-serviced reinforced concrete buildings, combined with environmental effects, lead to reinforcement corrosion. This situation becomes particularly critical for reinforced concrete structures exposed to wetting–drying cycles.

6.2. Concrete quality and corrosion of the in-service reinforced concrete building stock in Erzincan

Bayata et al. (2025) [116] conducted the seismic condition assessment of 3,199 buildings in Erzincan Province. In the study, using the "Street Screening Method" (Sucuoğlu, 2007) [117] and considering the Law No. 6306 on the Transformation of Areas Under Disaster Risk (ARAADHK), it was determined that 470 buildings were at high risk. It was reported that these structures exhibited low concrete quality and reinforcement corrosion, and it was recommended that urban transformation should be initiated urgently in these buildings.

Some thesis studies have also emphasized the corrosion mechanism in 25-45 years structures (see in Fig. 22) within the existing building stock in Erzincan [118, 119].

Figure 22. Corroded structural members in Erzincan province [118, 119]

7. Conclusion

This study comprehensively investigated the effects of natural corrosion on a reinforced concrete structure at the end of its service life, the mechanical behavior of the corroded reinforcement bars and concrete material, and the environmental effects. The following conclusions were obtained:

• Following mechanical and chemical cleaning, the actual corrosion ratios of the reinforcement bars were found to range between 6.33% and 25.57%, indicating significant material deterioration.

• Tensile test results indicated that pitting corrosion significantly reduced the mechanical properties compared to uniform corrosion. In accordance with these findings, reinforcement bars extracted from the building and whose actual corrosion ratios were determined generally exhibited pitting corrosion–induced cross-sectional loss at higher corrosion ratios.

• The average compressive strength of the concrete was 7.16 MPa, which was well below the minimum strength limits specified in the seismic design codes of 1975, 1998, 2007, and 2018.

• UPV test results confirmed that the concrete exhibited a heterogeneous microstructure, which further confirmed its poor mechanical quality.

• The strong correlation between field and laboratory UPV measurements (R^2 = 0.93) validated the reliability of in-situ testing methods in assessing concrete quality in old RC structures.

• Considering the long-term climate and air quality data of Erzincan province (1982–2017),

it has been revealed that seasonal changes in relative humidity values (35–85%), frequent freeze–thaw cycles, SO_2 concentrations generally below 50 µg/m³, and PM_{10} concentrations (up to 120 µg/m³) in winter months may have accelerated the corrosion mechanism. Therefore, the atmosphere of Erzincan is medium corrosive (C3 according to ISO 9224) during most of the year and highly corrosive (C4 according to ISO 9224) during the winter months. This effect was particularly significant in structures with inadequate concrete cover.

• The structure as a whole did not meet both the old and current specification requirements for seismic safety, indicating inadequate material quality and concrete cover thickness.

Article Information Form

The Declaration of Conflict of Interest/ Common Interest

No conflict of interest or common interest has been declared by authors.

Artificial Intelligence Statement

No artificial intelligence tools were used while writing this article.

Copyright Statement

References

[1] J. Y. Hu, S. S. Zhang, E. Chen, W. G. Li, "A review on corrosion detection and protection of existing reinforced concrete (RC) structures," Construction and Building Materials, vol. 325, p. 126718, 2022.

[2] M. Otieno, J. Ikotun, Y. Ballim, "Experimental investigations on the influence of cover depth and concrete quality on time to cover cracking due to carbonation-induced corrosion of steel in RC structures in an urban, inland environment," Construction and Building Materials, vol. 198, pp. 172-181, 2019.

[3] A. İ. Turan, Y. Ayaz, H. Yalciner, A. Kumbasaroglu, "An experimental evaluation on structural performance level of corroded reinforced concrete frames," Engineering Structures, vol. 325, p. 119479, 2025.

[4] D. Landolt, Corrosion and surface chemistry of metals. EPFL Press, 2007.

[5] S. A. Farooq, A. Raina, M. I. Haq, A. Anand, "Corrosion behaviour of engineering materials: A review of mitigation methodologies for different environments," Journal of The Institution of Engineers (India): Series D, vol. 103, no. 2, pp. 639–661, 2002.

[6] M. G. Fontana, Corrosion Engineering, Tata McGraw-Hill Education, 2005.

[7] F. Di Carlo, A. Meda, Z. Rinaldi, "Numerical evaluation of the corrosion influence on the cyclic behaviour of RC columns," Engineering Structures, vol. 153, pp. 264–278, 2017.

[8] S. Harsimran, K. Santosh, K. Rakesh, "Overview of corrosion and its control: A critical review," Proceedings on Engineering Sciences, vol. 3(1), pp. 13–24, 2021.

[9] Z. Ahmad, Principles of Corrosion Engineering and Corrosion Control, Elsevier, 2006.

[10] D. I. Răuță, E. Matei, S. M. Avramescu, "Recent development of corrosion inhibitors: types, mechanisms, electrochemical behavior, efficiency, and environmental impact," Technologies, vol. 13, no. 3, p. 103, 2025.

[11] E. L. Colvin, "Aluminum alloys: Corrosion," Encyclopedia of Materials: Science and Technology, 2001, pp. 107–110.

[12] Y. Ding, "Dealloyed nanoporous metals for catalysis," Reference Module in Materials Science and Materials Engineering, 2016.

[13] C. Frayne, Environmental Modification for Cooling, Heating and Potable Water Systems, 2010.

[14] Z. P. Bazant, "Physical model for steel corrosion in concrete sea structures-theor," ASCE Journal of Structural Engineering, vol. 105, no. 6, pp. 1137–1153, 1979.

[15] V. Kumar, N. Sharma, S. K. Tiwari, S. Kango, "Atmospheric corrosion of materials and their effects on mechanical properties: A brief review," Materials Today: Proceedings, vol. 44, pp. 4677–4681, 2021.

[16] X. Li, D. Zhang, Z. Liu, Z. Li, C. Du, C. Dong, "Materials science: Share corrosion data," Nature, vol. 527, no. 7579, pp. 441–442, 2015.

[17] P. R. Roberge, R. D. Klassen, P. W. Haberecht, "Atmospheric corrosivity modeling – a review," Materials & Design, vol. 23, pp. 321–330, 2002.

[18] B. Chico, D. Fuente, I. Díaz, J. Simancas, M. Morcillo, "Annual atmospheric corrosion of carbon steel worldwide. An integration of Isocorrag, Icp/Unece and Micat databases," Materials, vol. 10, no. 6, p. 601, 2017.

[19] D. C. Kong, C. F. Dong, Y. H. Fang, K. Xiao, C. Y. Guo, G. He, et al., "Long-term corrosion of copper in hot and dry atmosphere in Turpan, China," Journal of Materials Engineering and Performance, vol. 25, pp. 2977–2984, 2016.

[20] M. Esmaily, M. Shahabi-Navid, J. E. Svensson, M. Halvarsson, L. Nyborg, Y. Cao, et al., "Influence of temperature on the atmospheric corrosion of the Mg-Al alloy AM50," Corrosion Science, vol. 90, pp. 420–433, 2015.

[21] W. Zhang, L. Tan, D. Ni, J. Chen, Y. C. Zhao, L. Liu, et al., "Effect of grain refinement and crystallographic texture produced by friction stir processing on the biodegradation behavior of a Mg-Nd-Zn alloy," Journal of Materials Science & Technology, vol. 35, no. 5, pp. 777–783, 2019.

[22] L. Veleva, M. Acosta, E. Meraz, "Atmospheric corrosion of zinc induced by runoff," Corrosion Science, vol. 51, pp. 2055–2062, 2009.

[23] K. G. C. Berkeley, S. Pathmanaban, Cathodic Protection of Reinforcement Steel in Concrete. 1990.

[24] B. Yu, J. Liu, B. Li, "Improved numerical model for steel reinforcement corrosion in concrete considering influences of temperature and relative humidity," Construction and Building Materials, vol. 142, pp. 175–186, 2017.

[25] M. N. Nguyen, X. Wang, R. H. Leicester, "An assessment of climate change effects on atmospheric corrosion rates of steel structures," Corrosion Engineering, Science and Technology, vol. 48, no. 5, pp. 359–369, 2013.

[26] F. Mansfeld, "Atmospheric corrosion," in Electrochemical and Optical Techniques for the Study and Monitoring of Metallic Corrosion, Dordrecht: Springer Netherlands, 1991, pp. 571–584.

[27] H. B. Peacock, R. L. Sindelar, P. S. Lam, "Temperature and humidity effects on the corrosion of aluminium-base reactor fuel cladding materials during dry storage," in Reduced Enrichment for Research and Test Reactors, Proc. XVIII Int. Meeting, 2004, pp. 23–23.

[28] F. K. Firat, "Mechanical properties of reinforcing steel in R/C: uncertainty analysis and proposal of a new material factor," Arabian Journal for Science and Engineering, vol. 41, no. 10, pp. 4019–4028, 2016.

[29] Q. Li, X. Xia, Z. Pei, X. Cheng, D. Zhang, K. Xiao, X. Li, "Long-term corrosion monitoring of carbon steels and environmental correlation analysis via the

random forest method," npj Materials Degradation, vol. 6, no. 1, p. 1, 2022.

[30] Z. Pei, X. Cheng, X. Yang, Q. Li, C. Xia, D. Zhang, X. Li, "Understanding environmental impacts on initial atmospheric corrosion based on corrosion monitoring sensors," Journal of Materials Science & Technology, vol. 64, pp. 214-221, 2021.

[31] E. Chen, C. G. Berrocal, I. Fernandez, I. Löfgren, K. Lundgren, "Assessment of the mechanical behaviour of reinforcement bars with localised pitting corrosion by digital image correlation," Engineering Structures, vol. 219, p. 110936, 2020.

[32] A. İ. Turan, A. Kumbasaroglu, H. Yalciner, Y. Ayaz, "Prediction of seismic performance levels of corroded RC frames based on crack width," Structures, vol. 76, p. 108860, 2025.

[33] Y. Liu, "Modeling the time-to corrosion cracking of the cover concrete in chloride contaminated reinforced concrete structures," Ph.D. dissertation, Dept. Civil. Eng., Virginia Polytechnic Institute and State University, 1996.

[34] P. P. Beaujean, S. R. Shaffer, F. Presuel-Moreno, M. Brogden, "Evaluation of the physical characteristics of reinforced concrete subject to corrosion using a poro-elastic acoustic model inversion technique applied to ultrasonic measurements," Journal of Infrastructure Preservation and Resilience, vol. 5, no. 1, p. 7, 2024.

[35] A. A. Torres-Acosta, S. Navarro-Gutierrez, J. Terán-Guillén, "Residual flexure capacity of corroded reinforced concrete beams," Engineering Structures, vol. 29, no. 6, pp. 1145-1152, 2007.

[36] H. Yalciner, O. Eren, S. Sensoy, "An experimental study on the bond strength between reinforcement bars and concrete as a function of concrete cover, strength and corrosion level," Cement and Concrete Research, vol. 42, no. 5, pp. 643-655, 2012.

[37] H. Lin, Y. Zhao, J. Ožbolt, H. W. Reinhardt, "Bond strength evaluation of corroded steel bars via the surface crack width induced by reinforcement corrosion," Engineering Structures, vol. 152, pp. 506-522, 2017.

[38] F. Tondolo, "Bond behaviour with reinforcement corrosion," Construction and Building Materials, vol. 93, pp. 926–932, 2015.

[39] A. A. Almusallam, A. S. Al-Gahtani, A. R. Aziz, "Effect of reinforcement corrosion on bond strength," Construction and Building Materials, vol. 10, no. 2, pp. 123–129, 1996.

[40] M. R. Esfahani, B. V. Rangan, "Local bond strength of reinforcing bars in normal strength and high-strength concrete (HSC)," Structural Journal, vol. 95, no. 2, pp. 96–106, 1998.

[41] M. H. Harajli, "Comparison of bond strength of steel bars in normal- and high-strength concrete," Journal of Materials in Civil Engineering, vol. 16, no. 4, pp. 365–374, 2004.

[42] H. Lin, Y. Zhao, "Effects of confinements on the bond strength between concrete and corroded steel bars," Construction and Building Materials, vol. 118, pp. 127–138, 2016.

[43] Y. Ma, Z. Guo, L. Wang, J. Zhang, "Experimental investigation of corrosion effect on bond behavior between reinforcing bar and concrete," Construction and Building Materials, vol. 152, pp. 240–249, 2017.

[44] W. P. Zhang, H. Chen, X. L. Gu, "Bond behaviour between corroded steel bars and concrete under different strain rates," Magazine of Concrete Research, vol. 68, no. 7, pp. 364–378, 2016.

[45] C. Wu, S. Yu, J. Liu, G. Chen, "Development and testing of hybrid precast steel-reinforced concrete column-

to-H shape steel beam connections under cyclic loading," Engineering Structures, vol. 211, p. 110460, 2020.

[46] R. K. Biswas, M. Iwanami, N. Chijiwa, K. Uno, "Effect of non-uniform rebar corrosion on structural performance of RC structures: A numerical and experimental investigation," Construction and Building Materials, vol. 230, p. 116908, 2020.

[47] S. Srivaranun, M. Akiyama, P. Bocchini, V. Christou, D. M. Frangopol, H. Fukushima, K. Masuda, "Effect of the interaction of corrosion pits among multiple tensile rebars on the reliability of RC structures: Experimental and numerical investigation," Structural Safety, vol. 93, p. 102115, 2021.

[48] I. Fernandez, C. G. Berrocal, "Mechanical properties of 30 year-old naturally corroded steel reinforcing bars," International Journal of Concrete Structures and Materials, vol. 13, pp. 1-9, 2019.

[49] R. François, I. Khan, V. H. Dang, "Impact of corrosion on mechanical properties of steel embedded in 27-year-old corroded reinforced concrete beams," Materials and Structures, vol. 46, pp. 899–910, 2013.

[50] I. Fernandez, J. M. Bairán, A. R. Marí, "Corrosion effects on the mechanical properties of reinforcing steel bars: fatigue and σ–ε behavior," Construction and Building Materials, vol. 101, pp. 772–783, 2015.

[51] H. Yalciner, S. Sensoy, O. Eren, "Effect of corrosion damage on the performance level of a 25-year-old reinforced concrete building," Shock and Vibration, vol. 19, no. 5, pp. 891–902, 2012.

[52] H. Yalciner, S. Sensoy, O. Eren, "Seismic performance assessment of a corroded 50-year-old reinforced concrete building," Journal of Structural Engineering, vol. 141, no. 12, p. 05015001, 2015.

[53] A. Dasar, D. Patah, H. Hamada, D. Yamamoto, Y. Sagawa, "Life performance of 40-year-old RC beams with different concrete covers and bar diameters in natural corrosion environments," Structures, vol. 46, pp. 2031–2046, 2022.

[54] Y. Lv, D. Niu, X. Liu, Y. C. Li, "Corrosion damage and life prediction of concrete structure in a 41-year-old steelworks," Materials, vol. 15, no. 17, p. 5893, 2022.

[55] H. Grosser, M. Baumbach, H. Berckhemer, B. Baier, A. Karahan, H. Schelle, F. Krüger, A. Paulat, G. Michel, R. Demirtas, S. Gencoglu, R. Yılmaz, "The Erzincan (Turkey) earthquake (Ms 6.8) of March 13, 1992 and its aftershock sequence," Pure and Applied Geophysics, vol. 152, pp. 465–505, 1998.

[56] Boğaziçi University Kandilli Observatory and Earthquake Research Institute. (2017). Earthquake catalog [Online]. Available: http://www.koeri.boun.edu.tr/sismo/2/deprem-bilgileri/buyuk-depremler/

[57] Kandilli Observatory and Earthquake Research Institute, Boğaziçi University, Kandilli Observatory and Earthquake Research Institute (KOERI). International Federation of Digital Seismograph Networks, 1971.

[58] N. S. Trivedi, M. S. Venkatraman, C. Chu, I. S. Cole, "Effect of climate change on corrosion rates of structures in Australia," Climatic Change, vol. 124, pp. 133–146, 2014.

[59] T.C. Çevre, Şehircilik ve İklim Değişikliği Bakanlığı. (2025). Hava Kalitesi İzleme İstasyonları [Online]. Available: http://www.havaizleme.gov.tr/

[60] J. A. Gilliland, "Thermal and shrinkage effects in high performance concrete structures during construction," Ph.D. dissertation, Dept. Civil Engineering, The University of Calgary, Calgary, 2022.

[61] A. Nishikata, Q. Zhu, E. Tada, "Long-term monitoring of atmospheric corrosion at weathering steel bridges by an electrochemical impedance method," Corrosion Science, vol. 87, pp. 80–88, 2014.

[62] L. Zhang, L. Sun, L. Dong, "Experimental study on the relationship between the natural frequency and the corrosion in reinforced concrete beams," Advances in Materials Science and Engineering, vol. 1, p. 9976738, 2021.

[63] F. Tariq, M. Gaikwad, P. Bhargava, "Analysis of behaviour of corroded RC beams exposed to elevated temperatures," Journal of Building Engineering, vol. 42, p. 102508, 2021.

[64] W. Shao, X. He, D. Shi, "Durability life prediction of RC piles subjected to localized corrosion in chloride environments," Engineering Failure Analysis, vol. 136, p. 106184, 2022.

[65] G. Guarnieri, B. Olivieri, G. Senna, A. Vianello, "Relative humidity and its impact on the immune system and infections," International Journal of Molecular Sciences, vol. 24, no. 11, p. 9456, 2023.

[66] E. Bastidas-Arteaga, F. Schoefs, M. G. Stewart, X. Wang, "Influence of global warming on durability of corroding RC structures: A probabilistic approach," Engineering Structures, vol. 51, pp. 259–266, 2013.

[67] I. Dehri, M. E. Erbil, "The effect of relative humidity on the atmospheric corrosion of defective organic coating materials: An EIS study with a new approach," Corrosion Science, vol. 42, no. 6, pp. 969–978, 2000.

[68] X. Wang, X. Li, X. Tian, "Influence of temperature and relative humidity on the atmospheric corrosion of zinc in field exposures and laboratory environments by atmospheric corrosion monitor," International Journal of Electrochemical Science, vol. 10, no. 10, pp. 8361–8373, 2015.

[69] F. Samie, J. Tidblad, V. Kucera, C. Leygraf, "Atmospheric corrosion effects of HNO3— influence of temperature and relative humidity on laboratory-exposed copper," Atmospheric Environment, vol. 41, no. 7, pp. 1374–1382, 2007.

[70] N. Van den Steen, H. Simillion, O. Dolgikh, H. Terryn, J. Deconinck, "An integrated modeling approach for atmospheric corrosion in presence of a varying electrolyte film," Electrochimica Acta, vol. 187, pp. 714–723, 2016.

[71] Y. Cai, Y. Xu, Y. Zhao, X. Ma, "Atmospheric corrosion prediction: A review," Corrosion Reviews, vol. 38, no. 4, pp. 299–321, 2020.

[72] S. D. Cramer, S. A. Matthes, B. S. Covino, S. J. Bullard, G. R. Holcomb, "Environmental factors affecting the atmospheric corrosion of copper," ASTM Special Technical Publication, vol. 1421, pp. 245–264, 2002.

[73] Temiz Hava Hakkı Platformu. (2020). Kara Rapor 2020: Hava Kirliliği ve Sağlık Etkileri [Online]. Available: https://www.temizhavahakki.com/kara-rapor/

[74] Erzincan Valiliği Çevre ve Şehircilik İl Müdürlüğü, Erzincan İl Çevre Durum Raporu. Erzincan, 2012.

[75] Erzincan Valiliği, 2011. Erzincan İli Çevre Durum Raporu, Erzincan Çevre İl Müdürlüğü, Erzincan, 268s.

[76] P. Polat, M. S. Altınbilek, "Erzincan'ın iklim özellikleri ile Erzincan'da kaydedilen uzun dönem (1930–2020) sıcaklık ve yağış verilerinin trend analizleri," Doğu Coğrafya Dergisi, vol. 26, no. 46, pp. 55–80, 2021.

[77] A. Yazar, D. Y. Karakoç, "Hava kirliliğine ilişkin Mahalli Çevre Kurulu kararlarının

yansıttıkları: kararsızlık üretimine karşı savunuculuk gereksinimi," Akdeniz İİBF Dergisi, vol. 21, no. 2, pp. 164–179, 2021.

[78] N. V. Rao, M. Rajasekhar, G. C. Rao, "Detrimental effect of air pollution, corrosion on building materials and historical structures," American Journal of Engineering Research, vol. 3, no. 3, pp. 359–364, 2014.

[79] ISO, Corrosion of Metals and Alloys—Corrosivity of Atmospheres—Classification, Determination and Estimation, ISO 9224. Geneva, Switzerland: International Organization for Standardization, 2012.

[80] J. M. Costa, M. Vilarrasa, "Effect of air pollution on atmospheric corrosion of zinc," British Corrosion Journal, vol. 28, no. 2, pp. 117–120, 1993.

[81] R. W. Revie, Uhlig's Corrosion Handbook, 2nd ed. New York, NY, USA: Wiley, 2000.

[82] E. Aladag, "The influence of meteorological factors on air quality in the province of Van, Turkey," Water, Air, & Soil Pollution, vol. 234, no. 4, p. 259, 2023.

[83] J. Li, B. Chen, A. M. S. Campa, A. Alastuey, X. Querol, J. D. Rosa, "2005–2014 trends of PM10 source contributions in an industrialized area of southern Spain," Environmental Pollution, vol. 236, pp. 570-579, 2018.

[84] J. Žibert, J. Cedilnik, J. Pražnikar, "Particulate matter (PM10) patterns in Europe: An exploratory data analysis using non-negative matrix factorization," Atmospheric Environment, vol. 132, pp. 217-228, 2016.

[85] World Health Organization. (2021). Ambient (outdoor) air pollution [Online]. Available: https://www.who.int/newsroom/factsheets/detail/ambient-(outdoor)-air-quality-and-health

[86] Ö. Zeydan, "2019 Yılında Türkiye'deki Partikül Madde (PM10) Kirliliğinin Değerlendirilmesi," Journal of the Institute of Science and Technology, vol. 11, no. 1, pp. 106-118, 2021.

[87] Y. Li, Z. Y. Liu, J. Y. Jiang, "Microstructure and macroscopic properties of low-carbon concrete subjected to elevated temperature: State-of-the-art review," Journal of Building Engineering, vol. 86, p. 108731, 2024.

[88] M. Benaicha, O. Jalbaud, A. H. Alaoui, Y. Burtschell, "Correlation between the mechanical behavior and the ultrasonic velocity of fiber-reinforced concrete," Construction and Building Materials, vol. 101, pp. 702–709, 2015.

[89] E. A. Whitehurst, "Soniscope tests concrete structures," Journal Proceedings, vol. 47, no. 2, pp. 433–444, Feb. 1951.

[90] TS EN ISO 15630-1, "Steel for the reinforcement and prestressing of concrete – test methods – part 1: Reinforcing bars, rods and wire," Turkish Standards Institute, 2019.

[91] B. S. EN 12390-5, Testing Hardened Concrete – Part 5: Flexural Strength of Test Specimens. British Standards Institution, 2009.

[92] F. K. Fırat, M. S. Yücemen, "Determination of reliability based new load and resistance factors for reinforced concrete structural members," 2014.

[93] American Society for Testing and Materials, "ASTM G1-03: standard practice for preparing, cleaning, and evaluating corrosion test specimens," ASTM, 2004.

[94] ASTM A370–08a, "Standard Test Methods and Definitions for Mechanical Testing of Steel Products," ASTM International, West Conshohocken, PA, 2008.

[95] H. Yalciner, A. Kumbasaroglu, A. K. El-Sayed, A. P. Balkis, E. Dogru, A. I. Turan, K. Bicer, "Flexural strength of corroded reinforced concrete beams," ACI Structural Journal, vol. 117, no. 1, 2020.

[96] ABYYHY, "Turkish Building Earthquake Code," Turkish Disaster and Emergency Management Presidency, 1975.

[97] TBEC, Turkish Building Earthquake Code. Turkish Ministry of Environment and Urbanization, Ankara, Türkiye, 2018.

[98] G. F. Kheder, "A two stage procedure for assessment of in situ concrete strength using combined non-destructive testing," Materials and Structures, vol. 32, no. 6, pp. 410–417, 1999.

[99] N. V. Mahure, G. K. Vijh, P. Sharma, N. Sivakumar, M. Ratnam, "Correlation between pulse velocity and compressive strength of concrete," International Journal of Earth Sciences and Engineering, vol. 4, no. 6, pp. 871–874, 2011.

[100] H. Sucuoğlu, A. Erberik, "Performance evaluation of a three-storey unreinforced masonry building during the 1992 Erzincan earthquake," Earthquake Engineering & Structural Dynamics, vol. 26, no. 3, pp. 319–336, 1997.

[101] J. O. Malley, M. Celebi, N. R. Tilford, A. M. Ansal, P. Gulkan, W. Mitchell, M. Erdik, D. Ballantyne, Erzincan, Turkey Earthquake of March 13, 1992 (EERI Special Earthquake Report). Earthquake Engineering Research Institute (EERI), 1992.

[102] R. Yarar, J. Eisenberg, F. Karadogan, A Preliminary Report on the Erzincan Earthquake, March 13, 1992.

[103] M. S. Williams, A. Pomonis, E. Booth, G. Vaciago, S. Ring, The Erzincan Turkey Earthquake of 13 March 1992: A Field Report by EEFIT. London, UK: EEFIT, 1992.

[104] S. Bargu, Ş. Ersoy, "13 Mart 1992 Erzincan Depremi ile ilgili jeolojik gözlemler ve bazı öneriler," Jeoloji Mühendisliği Dergisi, vol. 16, no. 2, pp. 70–83, 1992.

[105] M. Erdik, Ö. Yüzügüllü, C. Yilmaz, N. Akkas, "13 March, 1992 (Ms = 6.8) Erzincan earthquake: A preliminary reconnaissance report," Soil Dynamics and Earthquake Engineering, vol. 11, no. 5, pp. 279–310, 1992.

[106] Boğaziçi University, March 13, 1992 (Ms = 6.8) Erzincan Earthquake: A Preliminary Reconnaissance Report. Boğaziçi University Press, May 1992.

[107] U. Ersoy, "Erzincan Depremi ve Betonarme Yapılar," in 13 Mart 1992 Erzincan Depremi Mühendislik Raporu, İnşaat Mühendisleri Odası Ankara Şubesi Yayını, Ankara, pp. 35–61, 1992.

[108] C. Kurtuluş, "13 March 1992 Erzincan earthquake and its results," in 2nd National Conference on Earthquake Engineering, 1993, pp. 310–318.

[109] A. Uğurlu, "Depremde beton ve davranışı," İMO Mühendislik Haberleri, vol. 476, no. 2, pp. 57–63, 2013.

[110] H. Tekel, "Erzincan ve Dinar'da yeniden yapılanmanın düşündürdükleri," Türkiye Mühendislik Haberleri, vol. 385, Sept. 1996.

[111] E. Akdağ, C. Karakurt, "Bilecik ilinde bulunan bazı özel ve kamu yapılarındaki beton özelliklerinin incelenmesi," Politeknik Dergisi, vol. 18, no. 1, pp. 1–6, 2015.

[112] L. Abosrra, A. F. Ashour, M. Youseffi, "Corrosion of steel reinforcement in concrete of different compressive strengths," Construction and Building Materials, vol. 25, no. 10, pp. 3915–3925, 2011.

[113] Y. Erbaş, Ö. Mercimek, Ö. Anıl, A. Çelik, S. T. Akkaya, İ. Kocaman, M. Gürbüz, "Design deficiencies, failure modes and recommendations for strengthening in reinforced concrete structures exposed to the February 6, 2023 Kahramanmaraş earthquakes (Mw 7.7 and Mw 7.6)," Natural Hazards, vol. 121, no. 3, pp. 3153–3194, 2025.

[114] A. C. Altunişik, M. E. Arslan, V. Kahya, B. Aslan, T. Sezdirmez, G. Dok, M. Nas, "Field observations and damage evaluation in reinforced concrete buildings after the February 6th, 2023, Kahramanmaraş–Türkiye earthquakes," Journal of Earthquake and Tsunami, vol. 17, no. 6, p. 2350024, 2023.

[115] O. Bozdogan, A. Erdag, A. Ozdemir, "Determination of mechanical properties of concrete and steel materials taken from buildings in Antakya after the Kahramanmaraş earthquakes," Case Studies in Construction Materials, vol. 21, p. e03445, 2024.

[116] H. F. Bayata, Y. E. Mazlum, F. İ. Baş, M. A. Çolak, "Erzincan kent merkezinin deprem güvenliği: yapı stoğu, ulaşım ağı, toplanma ve geçici barınma alanlarının stratejik analizi," Geomatik, vol. 10, no. 1, pp. 34–44, 2025.

[117] H. Sucuoğlu, U. Yazgan, A. Yakut, "A screening procedure for seismic risk assessment in urban building stocks," Earthquake Spectra, vol. 23, pp. 441–458, 2007.

[118] A. İ. Turan, "Paslanmaya maruz kalmış betonarme kirişlerin burulma dayanımı," Master's thesis, Erzincan Binali Yıldırım University, Institute of Science, 2019.

[119] M. F. Mermit, "Korozyona maruz kalmış tam ölçekli betonarme kolonlarda aderans-kayma ilişkisinin deneysel olarak incelenmesi," Master's thesis, Erzincan Binali Yıldırım University, Institute of Science, 2019.